JOURNAL OF MATERIALS SCIENCE 25 (1990) 3415–3423

Mechanical behaviour of magnetite from the Oconee-2 and TMI-1 steam generators using miniaturized specimen technology

M. P. MANAHAN
The Pennsylvania State University, 231 Sackett Building, University Park, PA, 16802, USA*

Flakes consisting primarily of iron oxide (magnetite) have been discovered in the spaces between tubes and support plates in steam generators, increasing flow resistance and causing abnormal increases in water levels. To determine the effects of tube scale on steam generators and to study the fracture and swelling behaviour of the flakes, Duke Power Company and MPR Associates, Inc. arranged for the author to measure the elastic modulus, fracture stress, and swelling of sludge from the steam generators of the Oconee Unit 2 (Oconee-2) and Three Mile Island Unit 1 (TMI-1) pressurized water reactors. The study measured the mechanical properties of the flakes directly, by deforming miniaturized specimens to fracture, rather than, for example, by deriving the properties by deflecting partially oxidized strip specimens, or by measuring the natural vibration frequency of a freely suspended rod during oxidation, as in past studies. Evidence indicates that the mechanical behaviour response of the Oconee-2 flakes is quite complex. The flakes are composed of multiple layers, each of which exhibits a different mechanical behaviour. Delamination during testing was observed, requiring special analytical treatment. The fracture stress of the strongest flake materials tested was in the range of 117 to 165 MPa. Thin, single-layered specimens exhibited moduli in the range of 137 880 to 227 502 MPa and layered specimens from 48 258 to 86 175 MPa at room temperature. The fracture stress of the TMI-1 flake materials tested was in the range of 20 to 114 MPa. There did not appear to be a substantial change in the range of stress at elevated temperatures. Unlike the Oconee-2 flakes, there was no evidence of delamination during bend testing.

1. Introduction

Tube scale that consists primarily of iron oxide (magnetite) may lodge in the spaces between the tubes and support plates in steam generators, increase flow resistance and cause abnormal increases in steam generator water levels. The hydrodynamic (water slap) process for cleaning scale from the tubes can be enhanced through preconditioning the scale by, for example, prewetting, predrying, or thermal cycling. Better understanding of the mechanical properties of the scale will permit more effective hydrodynamic cleaning. Models have been developed that describe flake transport, plugging, and the loads required to clear the blockage [1].

The author used patented miniature specimen technique [2] to measure important specimen properties such as elastic modulus, fracture stress and swelling, which can be used in the models in [1]. Much of the work on fracture strains of oxide films has been carried out using partially oxidized strip specimens [3–6]. Attempts have been made to derive mechanical property data from measurements of the natural vibration frequency of a freely suspended rod during oxidation and from the fracture strains of growing surface oxide scales under an externally applied tensile stress [1, 7–11]. There are no data in the literature on the fracture stress of Fe_3O_4. To the best of the author's knowledge, the present study is unique in that it is the first attempt to measure mechanical properties of thin flakes directly by deforming miniaturized specimens to fracture. Studies of the thermal expansion, thermal conductivity and curling behaviour of the Oconee-2 flake specimens are reported by Manahan [12].

2. Metallography, chemistry and specimen preparation

2.1. Metallography

Sludge from the Oconee-2 generator was sorted and the largest flakes were removed for metallographic investigation and specimen preparation. Metallographic studies were conducted to determine the microstructure of the flakes, and to determine if anisotropy occurs in the plane normal to the tube radius. The flakes were found to be reasonably isotropic. Photomicrographs were made both before (as-polished) and after etching. The average grain size near the centre of the cross section was determined to be 0.005 mm as shown in Figs 1 and 2. Near the outside diameter (OD) surface, grains as large as 0.01 mm were observed. Hence a minimum specimen

*The work was performed during employment at Battelle.

0022–2461/90 $03.00 + .12

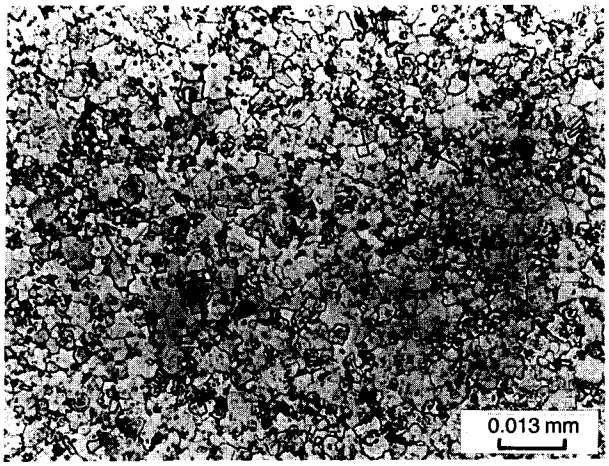

Figure 1 Microstructure of Oconee-2 magnetite flake near centre of cross section.

dimension of about 0.1 mm is required for continuum behaviour. The majority of flakes tested met the continuum thickness requirement.

An important difference was observed between the surface morphologies of the flake inside diameter (ID) and OD surfaces. The ID surfaces were noticeably smoother, with linear striations oriented in the circumferential direction of the tubes. The OD surfaces were rougher and porous in appearance. Photomicrographs of the flake cross section confirmed that the outer surfaces showed appreciable porosity (see Fig. 2). The etchant used was 45% H_2O, 30% HCl, 20% HNO_3 and 5% HF.

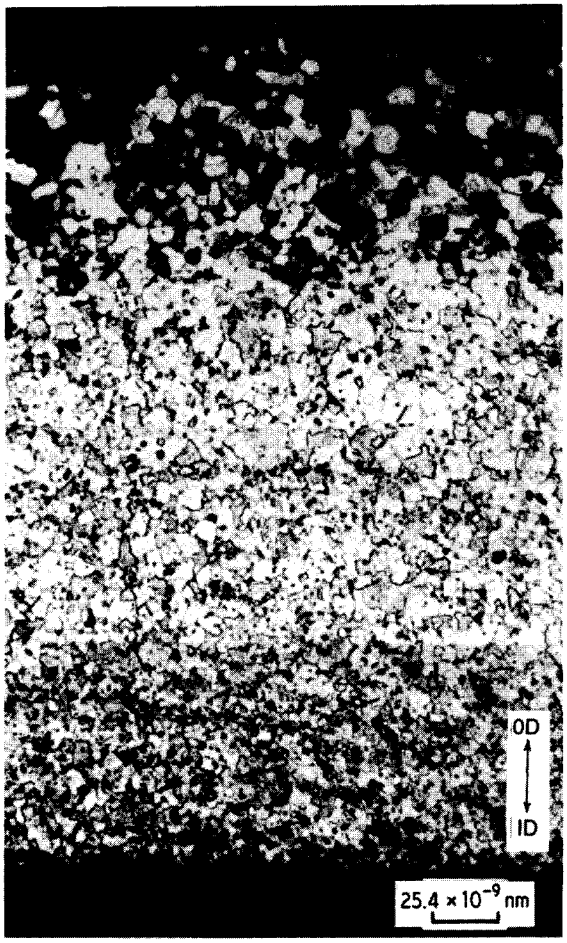

Figure 2 Photomontage of Oconee-2 magnetite flake, showing increased porosity toward the OD surface.

There appear to be three groups of grain size for the Oconee-2 flake shown in Fig. 2. The small grains are located near the ID surface and extend through approximately one-third the thickness of the flake. The intermediate size grains are located in the central portion of the cross section and extend over a distance of approximately one-half of the specimen thickness. The largest grains are located in the porous region near the tube OD surface. The number and thickness of the regions vary widely from flake to flake. A photomicrograph of a flake sectioned parallel to the tube axis in the as-polished condition is shown in Fig. 3. Copper-coloured particles were observed in the material. Further work is needed to determine the particle compositions.

A similar investigation was conducted for the TMI-1 flakes. All the specimens investigated had at most two layers, with one exception. The criterion used to judge the number of layers present in the specimens was an abrupt change in the average grain size [2, 13]. Figures 4–6 show representative photomicrographs of the TMI-1 flake specimens. Figure 5 shows a two-layered specimen that is evident from the large-diameter grains near the inner diameter and smaller grains near the outer diameter surface. All of the specimens examined after polishing had particles which were possibly copper-rich [13] (Fig. 3). Evidence of a possible glassy phase in the TMI-1 specimens was also observed during the light microscopy investigation. Specimen G9 appeared to have a different material near the centre of the cross section. The material was removed after etching.

2.2. Chemistry

Chemical and physical analysis of the Oconee-2 sludge flakes was performed by Duke Power Company and Combustion Engineering [14, 15]. The flakes were found to be nearly identical in chemical composition, and they consisted of nearly pure iron oxide (as magnetite, Fe_3O_4). The concentration ranged from 68 to 70 wt % Fe. All other elements had concentrations < 1 wt %. Methods used to determine elemental composition included X-ray fluorescence, CHN analysis,

Figure 3 Oconee-2 magnetite in the as-polished condition sectioned parallel to the tube axis. White areas are copper-coloured particles.

Figure 4 Photomicrograph of TMI-1 specimen G3 showing single layer of large grain intermixed with small grain.

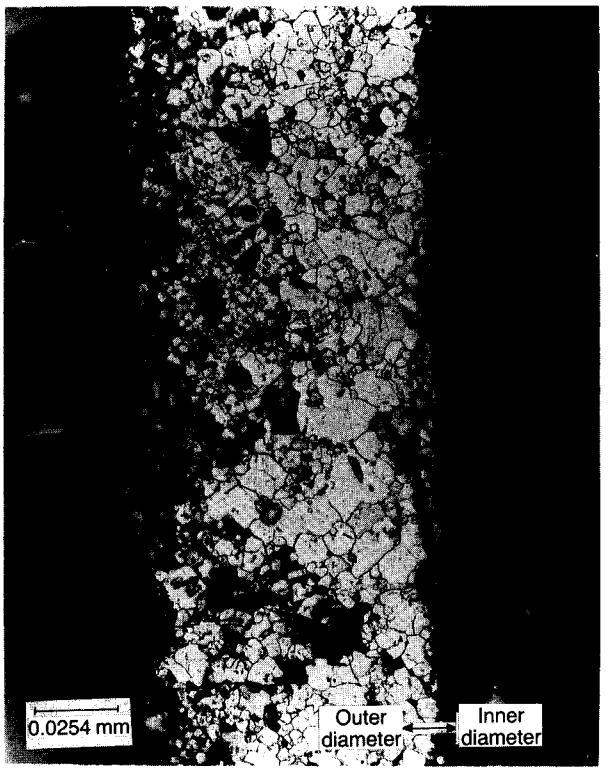

Figure 5 Photomicrograph of TMI-1 specimen G6 showing two layers and increasing porosity near the outer diameter surface.

and emission spectroscopy. X-ray diffraction analysis indicated that magnetite is the only polycrystalline form of iron occurring in the sludge [15]. One sample was powdered for leaching analysis by ion chromatography and atomic absorption. Calcium, sodium, sulphate and magnesium were the most prevalent leachable components, with concentrations ranging from 18.1 to 4.0 p.p.m. Other components, all at < 2.5 p.p.m., were present. Table I indicates the results of the elemental analysis conducted on large flake and small flake samples, while Table II shows the chemical analysis for leachable sample components [15]. Samples were also measured for sludge density by several methods: apparent bulk, tap, and water displacement/immersion. Table III shows the sludge density measurement results [15].

TABLE I Oconee-2 steam generator sludge sample elemental analysis.*

Element	Small flake sample†	Large flake sample†
Iron	70	68
Manganese	1	1
Silicon	0.11‡	1
Chromium	1	< 1.0¶
Molybdenum	0	0
Zinc	0	0
Copper	0	0
Potassium	0	0
Nickel	0	0
Chlorine	0	0
Sulphur	0	0
Titanium	0	0
Calcium	0	< 1.0¶
Phosphorus	0	0
Aluminium	0	< 1.0¶
Lithium	< 10 p.p.m.‡	< 10 p.p.m.‡
Boron	< 10 p.p.m.‡	< 10 p.p.m.‡
Sodium	0.002‡	0.02‡
Magnesium	0.07‡	0.41‡
Carbon	< 0.3§	< 0.3§
Hydrogen	< 0.1§	< 0.1§
Nitrogen	< 0.1§	< 0.1§

*Analysis by X-ray fluorescence except as noted.
†Values provided in weight percent except as noted.
‡Analysis by emission spectroscopy.
§Analysis by Perkin Elmer 240 carbon, nitrogen, hydrogen analyser.
¶Identified in trace amount.

2.3. Specimen preparation

The Oconee-2 sorted flakes were found to be irregular in shape with typical dimensions in the axial direction (parallel to the tube axis) of 3.81 to 5.08 mm, along the circumferential direction of about 2.54 mm and from 0.1 to 0.2 mm in thickness. The TMI-1 flakes had comparable planar dimensions; however, the thickness ranged from 0.0470 to 0.108 mm.

For the determination of elastic modulus and fracture stress, the flakes were machined into curved

TABLE II Oconee-2 steam generator sludge sample chemical analysis for leachable sample components

Leachable component	Analysis	Concentration in sludge of leachable portion (p.p.m.)
Cl	Ion chromatography	2.5
PO_4	Ion chromatography	< 0.5
NO_3	Ion chromatography	1.4
SO_4	Ion chromatography	5.8
Li	Atomic absorption	< 2.0
Mg	Atomic absorption	4.0
Na	Atomic absorption	7.2
Cu	Atomic absorption	< 2.0
K	Atomic absorption	< 2.0
Ca	Atomic absorption	18.1

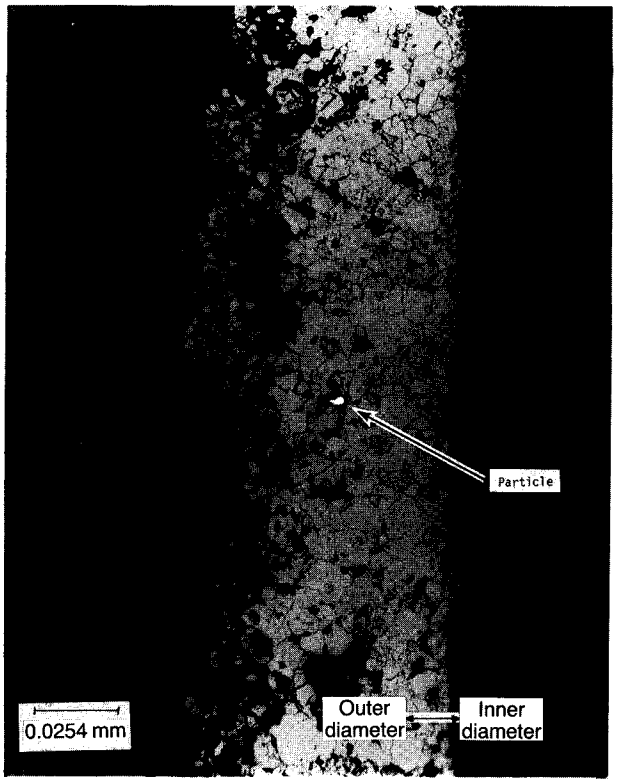

Figure 6 Photomicrograph of TMI-1 specimen G7 showing a particle that remained after etching.

beams that were tested in a four-point bend fixture. For tests of swelling, flakes were machined into thin, straight beams. The bend specimens were machined so that their length dimension was parallel to the hoop direction of the Inconel tubes, while the swelling specimens were oriented so that their length was parallel to the tube axis.

As a consequence of the dimensions of the flake samples received, the length of the bend test specimens was nominally 2.54 mm, while the length of the swelling specimens was up to 5.08 mm. The bend specimens were machined to a nominal width of 1.91 mm and the swelling specimens had a nominal width of 1.27 mm.

3. Test methods, analysis and results

3.1. Elastic modulus and fracture stress

A four-point static bend test measured the modulus and fracture stress. For a brittle material such as magnetite, four-point bend loading is preferable to three-point loading. A brittle specimen in a three-point bend test may not fracture at the point of maximum bending moment, that is, at the point of load application. However, in a four-point bend test, the entire region between the two loading points is at a constant maximum value of bending moment. Provided the test specimen fractures between the two load points, a constant value of maximum bending moment may be used in the equations for fracture strength and modulus.

TABLE III Oconee-2 steam generator sludge density measurements

Type of density	$g\,cc^{-1}$
Apparent bulk	1.70
Tap	2.01
Average immersion	4.16

The bend tests were performed at room temperature (RT) and at 288° C and the load was increased continuously. Since the nominal length of the bend specimens was 0.3 cm, the specimen support was designed to allow a distance of 0.2 cm between supports, giving the test beam an overhang of at least 0.03 cm on either side of the support. A one-piece specimen loading punch, designed with twin blades 0.10 cm apart, slid in grooves machined in the specimen support fixture. Because the specimens were small and the dimensional tolerances had to be maintained at the test temperature, the specimen support and loading punch were machined from Invar.

Figure 7 shows a schematic drawing of the loading apparatus. The specimen's support block rests on a heated stage that can be moved in the x–y direction by micrometer drives. The load arm is pressed against the specimen punch by a pneumatic actuator, and this load is reacted through a precision load cell. The rate of load application iron is determined using an adjustable leak in the pneumatic system, actuated by opening and closing an exhaust valve. The bend test used a rate of load application of $\sim 4.7\,kg\,min^{-1}$.

3.2. Analysis

The exact value of bending moment at the point of fracture must be known to evaluate the fracture strength of the material from flexure equations. Several four-point bend stress/strain relationships were examined for accuracy in analysing the experimental data [13]. Each model is briefly described in turn below.

3.2.1. Straight-beam (flat plate) solution

As discussed by Singer [16], the double-integration method can be used to derive the following relationships:

$$E = \frac{Pa[3L^2 - 4a^2]}{2\delta wh^3} \quad (1)$$

$$\sigma_{max} = \frac{6Pa}{wh^2} \quad (2)$$

where E = elastic modulus; P = load applied to each punch blade; d = punch blade span; L = support span; $a = (L - d)/2$; δ = specimen mid-point deflection; w = specimen width; h = specimen thickness and σ_{max} = maximum tensile stress.

3.2.2. Hyperbolic stress distribution approximation

In general, a stressed initially curved beam differs from a stressed straight beam in the following ways:

1. There is an increase in the stresses toward the inner (concave) side and a decrease toward the outer (convex) side. This results in an asymmetric stress distribution across the beam section.
2. In order to maintain equilibrium, the neutral axis no longer passes through the centroid of the cross section, but is shifted towards the concave or inner side.

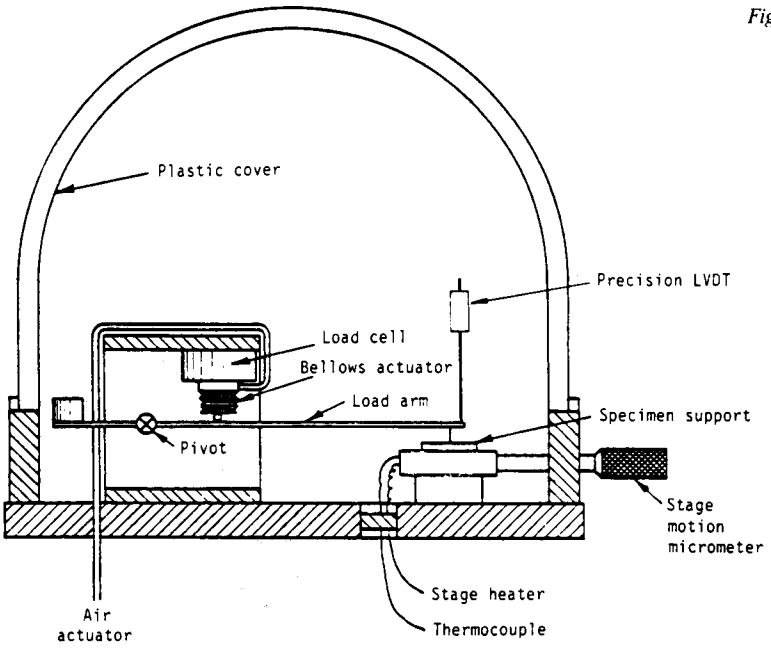

Figure 7 Schematic drawing of the bend test apparatus.

For cross sections of simple geometry, it is possible to find the location of the neutral axis. It can be shown [17] for a rectangular cross section of depth h and width w and inner and outer radii of r_i and r_o, respectively, that the radius of the neutral axis $r_{n\cdot a}$ is given by:

$$r_{n\cdot a} = \frac{h}{\ln\left(\frac{r_o}{r_i}\right)} \tag{3}$$

If r_c is the radius to the centroid of the cross-sectional area, the maximum stress (which occurs on the inside surface) is given by Shanley [17]:

$$\sigma_{max} = \frac{Mc}{Ar_i(r_c - r_{n\cdot a})} = \frac{Pa(r_{n\cdot a} - r_i)}{whr_i\left[r_c - \frac{h}{\ln\left(\frac{r_o}{r_i}\right)}\right]} \tag{4}$$

where M = bending moment; $c = r_{n\cdot a} - r_i$ and $A = wh$. For a straight beam, the maximum stress is given by

$$\sigma_{max} = \frac{6M}{wh^2} \tag{5}$$

The ratio of these maximum stresses can be given by a correction factor K where

$$K = \frac{\sigma_{max}(\text{curved})}{\sigma_{max}(\text{straight})} \tag{6}$$

3.2.3. Exact solution for an initially curved beam in pure bending

For a curved beam of width unity, an inner radius r_i, an outer radius r_o and pure moments M applied at the ends, the solution is provided by Timoshenko and Goodier [18]. The expressions for radial stress σ_r, tangential stress σ_θ and shear stress $\tau_{r\theta}$ are

$$\sigma_r = \frac{A}{r^2} + B(1 - 2\ln r) + 2C \tag{7}$$

$$\sigma_\theta = \frac{-A}{r^2} + B(3 + 2\ln r) + 2C \tag{8}$$

$$\tau_{r_\theta} = 0 \tag{9}$$

where A, B and C are constants to be determined from the boundary conditions of the system. Application of the boundary conditions yields

$$A = -\frac{4M}{N} r_i^2 r_o^2 \ln\left(\frac{r_o}{r_i}\right) \tag{10}$$

$$B = -\frac{2M}{N}(r_o^2 - r_i^2) \tag{11}$$

$$C = \frac{M}{N}[r_o^2 - r_i^2 + 2(r_o^2 \ln r_o - r_i^2 \ln r_i)] \tag{12}$$

where

$$N = (r_o^2 - r_i^2)^2 - 4r_o^2 r_i^2 \left(\ln\frac{r_o}{r_i}\right)^2 \tag{13}$$

Substituting these into the stress equations

$$\sigma_r = -\frac{4M}{N}\left(\frac{r_i^2 r_o^2}{r^2}\ln\frac{r_o}{r} + r_o^2 \ln\frac{r}{r_o} + r_i^2 \ln\frac{r_i}{r}\right) \tag{14}$$

$$\sigma_\theta = -\frac{4M}{N} \times \left(-\frac{r_i^2 r_o^2}{r^2}\ln\frac{r_o}{r_i} + r_o^2 \ln\frac{r}{r_o} + r_i^2 \ln\frac{r_i}{r} + r_o^2 - r_i^2\right) \tag{15}$$

For a bar of width w, the above expressions would have w in the denominator.

Since the beams are initially curved, the flat plate solution was compared with the curved beam solutions using both the hyperbolic stress distribution approximation and the exact solution for an initially curved beam in pure bending. Since the difference between the flat plate and curved beam solutions is small for the geometry of interest ($\sim 1\%$), the flat plate equations were used to analyse the data. In all

TABLE IV Bench-mark data for miniature four-point test performed on porcelain specimens

Specimen identification	Miniature specimens		Large specimens	
	Maximum stress (MPa)	Elastic modulus (MPa) (bending)	Maximum stress (MPa)	Elastic modulus (MPa)
PORC1	51	47086	–	–
PORC2	42	46191	–	–
PORC6	56	58945	–	–
PORC8	47	50878	–	–
PORC10	38	41640	–	–
Average	47	48947	72 (bend)	71088 (uniaxial compression) 73076 (pulse/echo)

tests, the load train compliance was measured (RT, 288° C) and the data were adjusted for compliance. The specimen pre-load (dead weight of the punch) was added to the recorded data. The measured punch, support and specimen dimensions after machining were used in the calculations.

3.3. Mechanical property results

Bench-mark bend test data using porcelain specimens machined to approximately the same dimensions as the flakes were compared with large specimen data. The miniature and large specimen data are compared in Table IV. The average miniature bend modulus is approximately 30% lower than the average large specimen modulus determined in compression. This difference is probably due to the measurement technique (bending as opposed to compression) and the uncertainty in the specimen thickness in the vicinity of the crack. The difference in the fracture stress is probably due to specimen thickness uncertainties, as well as the effects of surface scratches in the miniature specimens. Although the specimens were polished, small scratches in the miniature specimens are likely to have a greater effect on fracture stress than in large specimens.

The miniature Oconee-2 flake data are presented in Tables V to VIII for the room temperature and 288° C tests. Specimens are identified by a four-character alpha-numeric sequence. The first character, M, indicates magnetite flakes. The second character is an arbitrary sequential number. The third character indicates whether the specimen was tested concave up (U) or concave down (D). The last character indicates whether the specimen was tested wet (W) at RT, dry (D) at RT, or dry at 288° C (T).

The Oconee-2 flake response under loading is very complex. Jogs in the load/deflection curve were observed for several of the specimens. The apparatus was checked and found to be performing properly, with no slippage in the load train. Visual examination of the fracture surface showed that the crack did not propagate straight through the thickness for all specimens. As shown in Fig. 8, some specimens exhibited fracture within the bulk material during testing, which resulted in a layered specimen. The crack plane was at times oriented in the hoop direction, which would explain the loss of stiffness that may have resulted in jogs in the load/deflection curve. However, not all specimens that were layered after testing had jogs in the load/deflection curve.

After testing, it was observed that portions of striations on the ID surface of several specimens were covered with a material that is similar to the OD surface material (Fig. 9). This may be relevant to the study of scale formation and transport. If the striations are an artefect of the tube machining revealed from flakes spalling off the tube, then the material found on the ID surface may have been deposited there after the flake was removed from the tube. Alternatively, the material could have attached during contact with the OD surface of other flakes (residual magnetism or chemical bonding).

Another explanation for the loss of stiffness during some tests is partial through-thickness cracking. However, this is unlikely because calculations indicate that

TABLE V Mechanical behaviour of Oconee-2 flakes at room temperature (20° C)

Specimen identification	Orientation	Condition	Maximum stress (MPa)	Flake modulus (MPa)	Specimen thickness (mm)	Maximum load (kg)	Number of jogs in load/deflection curve	Number of layers optically observed in fracture surface	Maximum stress with porosity correction (MPa)	Flake modulus with porosity correction (MPa)
M2UD	Concave up	Dry	73	186758	0.101	0.094	0	1 (clean break)	71	179864
M1UD	Concave up	Dry	69	51705*	0.116	0.111	0	2 (clean break)	135	140569
M10UW	Concave up	Wet	61	80039	0.137	0.142	0	3	54	66320
M12UW	Concave up	Wet	50	42536	0.181	0.213	0	1 (clean break)	52	43984
M8UD	Concave up	Dry	27	45018	0.198	0.133	1	2	41	82590
M3DD	Concave down	Dry	77	126022	0.137	0.131	0	3	85	146153
M5DW	Concave down	Wet	88	126574	0.151	0.169	2	2 (clean break)	131	229432
M13DD	Concave down	Dry	29	49430	0.201	0.105	3	3	42	86244

*First test to define load/displacement range. Modulus is approximate due to non-linear compliance.

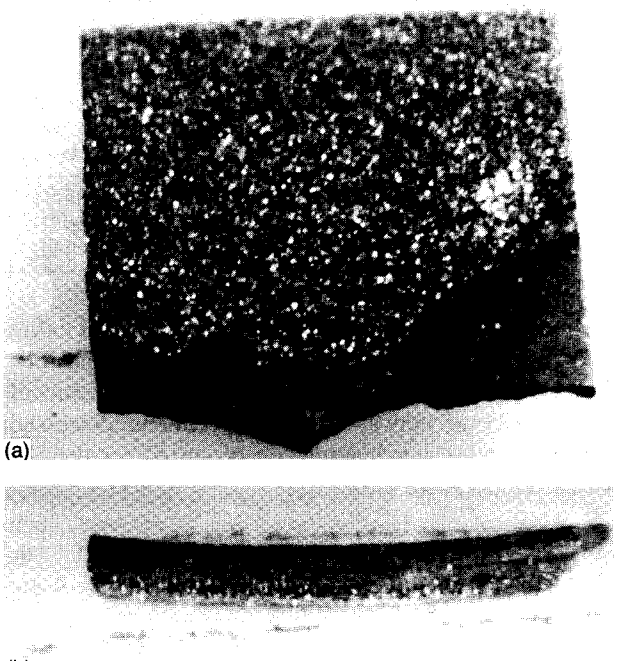

Figure 8 Fracture surface of Oconee-2 specimen M13DD.

Figure 9 ID surface of specimen M10UW after wet testing.

cracking of the layers would result in stresses high enough to crack the remaining ligament. In future experiments, after a jog in the curve is observed, it would be helpful to stop the test, section the specimens, determine if a crack is present in the material, and observe the orientation of the crack (hoop or through-thickness).

As mentioned earlier, the Oconee-2 metallographic analysis supports the explanation of internal hoop-oriented cracking. Figure 2 shows three groupings of grain size that change fairly abruptly through the thickness. From a mechanical behaviour viewpoint, it is as if there are three different materials laminated together. In addition, Hairston and Frye [14] reported chemical variations through the thickness of some flakes. As stated by Szlarska-Smialowska [19], magnetite has been observed to form in layers and/or have a chemical gradient through the thickness. Individual materials in the layers could be studied by separating the layers after testing. Useful tests would include chemical analysis, X-ray diffraction and metallography.

As a result of these observations it is not possible to report an elastic modulus in the conventional sense. The elastic modulus is a measure of the displacement of atoms from their equilibrium positions in a given material. Since a given flake may have compositional variation through the thickness and varying grain sizes (indicating different mechanical response within each layer), a 'flake modulus' is reported that is calculated based on the initial slope of the load deflection curve. As a result of these considerations, large variations in the flake modulus are to be expected, as shown in Tables V to VIII. As shown in Tables VI and VIII, the layer thicknesses were measured at the fracture surfaces of each specimen and the results based on the nominal pretest thickness measurements were corrected.

The high level of porosity in the OD surface layer indicates that this layer has negligible load carrying capacity. Therefore, in Tables V and VII, the stress

TABLE VI Mechanical behaviour of Oconee-2 flakes at room temperature corrected for specimen thickness

Specimen ID	Layer 1 (ID surface) thickness (mm)	Layer 2 thickness (mm)	Porous layer (OD surface) thickness (mm)	Comments	Maximum stress with specimen thickness correction (MPa)
M2UD	0.103	–	Not measurable	Clean break	71
M1UD	0.0828	–	0.021	Clean break	135
M10UW	~0.11	~0.0371	~0.016	ID/OD surfaces not parallel; striations covered by black material	96
M12UW	0.179	–	Not measurable	Clean break; rough OD surface	52
M8UD	0.0815	0.0805	0.012	No evidence of striations	162
M3DD	0.020	0.111	0.014	Faint evidence of striations	118
M5DW	0.124	–	0.0262	Clean break; striation partly covered; OD layer rough	131
M13DD	0.103	0.0640	0.0361	OD layer very rough; almost no evidence of striations on ID surface	111

TABLE VII Mechanical behaviour of Oconee-2 flakes at 288° C

Specimen identification	Orientation	Condition	Maximum stress (MPa)	Flake modulus (MPa)	Specimen thickness (mm)	Maximum load (kg)	Number of jogs in load/deflection curve	Number of layers optically observed in fracture surface	Maximum stress with porosity correction (MPa)	Flake modulus with porosity correction (MPa)
M4DT	Concave down	Dry	95	65 286	0.133	0.106	1	1	117	88 519
M7UT	Concave up	Dry	96	166 766	0.166	0.166	0	1	97	168 972
M9UT	Concave up	Dry	70	125 747	0.127	0.140	1	1	52	79 695

and flake moduli were recalculated by using the specimen thickness at fracture and subtracting the thickness of the porous layer from the overall specimen thickness. After this data correction, there is a distinct trend in the data of a decrease in flake modulus with increasing thickness. The thin, single-layered specimens tested at RT exhibit moduli (140 569 to 229 432 MPa) that are comparable to handbook data for magnetite (227 502 MPa).

In Tables VI and VIII, a further correction was applied to the fracture stress data. It is postulated that prior to testing the layers are continuous and, at a certain load, the layers separate in the central portion of the flakes. Although the stress field in the layered specimens is fairly complex, a simple correction can be applied to estimate the fracture stress in the material. The following corrections were made to the fracture stress data:

1. The actual thickness of the layers at the fracture surface was used in the stress calculation.
2. The porous layer does not carry any load.
3. For specimens containing two non-porous layers, only the thickest layer is used in the stress computation.

As shown in Tables VI and VIII, these corrections bring the data into more consistent agreement. There appear to be two distinct materials present at room temperature: one with a fracture stress in the range of 117 to 165 MPa for specimens of thickness 0.081 to 0.12 mm; the second with a fracture stress in the range of 51.7 to 110.3 MPa for specimens of thickness 0.1 to 0.2 mm. A similar trend is observed for the high-temperature tests.

The miniature TMI-1 flake data are presented in Tables IX and X. There was no evidence of delamination in these tests. Since the width of the outer layer varied significantly and the OD layer of the TMI-1 flakes was not as porous as the Oconee-2 flakes, no porous layer correction was applied to the TMI-1 data. For the TMI-1 flakes, the modulus ranged from 25 783 to 72 593 MPa and the maximum stress ranged from 21 to 114 MPa at room temperature. Therefore the TMI-1 modulus is significantly lower than that for Oconee-2, whereas the stress ranges for the TMI flakes and the weaker Oconee-2 material are comparable. The low moduli results for TMI-1 may be a result of the impact of flaws on thin specimens discussed earlier. Similar conclusions can be stated for the elevated temperature data.

3.4. Swelling results

A Sheffield Accutron Model 50185 vertical comparator was used for swelling measurements on the Oconee-2 flakes, which were made in a temperature- and humidity-controlled laboratory. The system is capable of length measurement with an uncertainty of $\pm 12.7 \times 10^{-6}$ mm. The room temperature was carefully controlled to 20 ± 0.6° C and the relative humidity was 39.4%. Calibration runs were made prior to taking measurements on a specimen. The calibration runs were necessary to account for the shortening of the stylus after distilled water was added. Readings were taken every half-hour for several hours. After subtracting the calibration curve for each specimen, there was no detectable swelling in the flakes. Since the measurement uncertainty is $\pm 12.7 \times 10^{-6}$, any swelling may be presumed to be below 0.0017%.

4. Conclusions

The mechanical behaviour response of the Oconee-2 flakes is quite complex. Evidence suggests that the flakes are composed of two or, for thicker flakes, three layers of material, each of which exhibits different mechanical properties. There does not appear to be any significant change in the mechanical behaviour of the flakes when tested wet. However, the data are sparse and there is considerable scatter due to the nature of the flakes and the fact that they were tested in the as-received condition.

For the Oconee-2 flakes, there appear to be two distinct materials present. At room temperature, the fracture stress of the strongest Oconee-2 flake materials tested was in the range of 117 to 165 MPa. The weaker material exhibited a fracture stress in the range of 51.7 to 110.3 MPa. There does not appear to

TABLE VIII Mechanical behaviour of Oconee-2 flakes at 288° C corrected for specimen thickness

Specimen ID	Layer (ID surface) thickness (mm)	Layer 2 (OD surface) thickness (mm)	Porous layer thickness (mm)	Comments	Maximum stress with specimen thickness correction (MPa)
M4DT	0.102	–	Not measurable	Broke into 4 pieces	117
M7UT	0.116	–	Not measurable	Broke into 3 pieces	97
M9UT	0.148	–	Not measurable	Broke into 4 pieces	52

TABLE IX Mechanical behaviour of flakes at room temperature (20° C)

Specimen identification	Orientation	Specimen thickness (mm)	Maximum stress (MPa)	Flake modulus (MPa)
G41U	Concave up	0.0975	50	38 330
G43U	Concave up	0.0958	47	42 398
G51U	Concave up	0.0881	77	25 783
G61D	Concave down	0.0992	114	99 963
G503D	Concave down	0.0899	21	72 593
G504D	Concave down	0.0767	42	30 057
Average	–	0.0900	59	51 521
Standard deviation	–	0.0074	33	28 883

be a substantial change in the range of stresses measured at elevated temperature. The thin, single-layered specimens tested at RT exhibited moduli of 137 880 to 227 502 MPa. The layered specimens and single-layer specimens exhibited moduli in the range of 48 258.0 to 86 175.0 MPa at RT. The flake swelling was below the measurement uncertainty. Therefore the swelling, if it occurs, is below 0.0017%.

As with the Oconee-2 flakes, the TMI-1 flakes were found to contain particles in the 0.003 mm size range. In the TMI-1 flakes, light microscopy revealed evidence of a possible glassy phase. With one exception, all of the TMI-1 flakes studied were either one- or two-layered as judged by abrupt changes in grain size. The thickness of the TMI-1 flakes studied ranged from 0.0470 to 0.108 mm, as compared with the relative thick Oconee-2 flakes which ranged from 0.1 to 0.2 mm.

The fracture stress of the TMI-1 flake materials tested was in the range of 20 to 114 MPa, which compares well with the weaker material in the Oconee-2 specimens. There did not appear to be a substantial change in the range of stresses measured at elevated temperatures. There was no evidence of delamination during bend testing.

TABLE X Mechanical behaviour of flakes at 288° C

Specimen identification	Orientation	Specimen thickness (mm)	Maximum stress (MPa)	Flake modulus (MPa)
G31U	Concave up	0.0714	42	43 225
G501U	Concave up	0.108	36	13 305
G62U	Concave up	0.0970	77	47 775
G502D	Concave down	0.0780	199*	367 588*
G506D	Concave down	0.0886	84	330 567†
G507D	Concave down	0.0993	79	113 613
Average	–	0.0904	64	54 480
Standard deviation	–	0.0138	23	42 284

*Data may not be valid due to probable fracture outside of punch span; average does not include these data.
†Modulus data are not valid due to irregular crack propagation; average does not include this datum.

Acknowledgements

The author wishes to acknowledge Duke Power Company and MPR Associates, Inc., for their support of the work reported here. Particular thanks for assistance and support are given to R. Eaker of Duke Power, J. Nestell and N. Cole of MPR Associates, and S. Giacobbe of GPU Nuclear. Special thanks also go to Battelle staff involved in the testing: N. Frey, C. Charles, D. Rider and J. Park.

References

1. J. ARMITT *et al.*, in "The Spalling of Steam-Grown Oxide from Superheater and Reheater Tube Steels" (Report to EPRI from Central Electricity Research Laboratories, February, 1978) p. 3-1.
2. M. P. MANAHAN, A. S. ARGON and O. K. HARLING, US Patent 4 567 774, February (1986).
3. E. M. FIELD, R. C. STANLEY, A. M. ADAMS and D. R. HOLMES, in Proceedings of the 2nd International Congress on Metal Corrosion New York, 1963 (Butterworth, London) p. 829.
4. P. L. HARRISON, *Corr. Sci.* 7 (1967) 789.
5. H. A. McCARTHY and P. L. HARRISON, *ibid.* **14** (1974) 469.
6. D. R. HOLMES and R. T. PASCOE, *Werk. u. Korr.* **10** (1972) 859.
7. D. BRUCE and P. HANCOCK, *J. Inst. Met.* **97** (1969) 148.
8. P. HANCOCK, *Werk. u. Korr.* **12** (1970) 1002.
9. P. HANCOCK and R. C. HURST, in "Advances in Corrosion Science and Technology", Volume 4, edited by M. G. Fontana and R. W. Staehle (Plenum, New York, 1974). p. 1-79.
10. R. C. HURST and P. HANCOCK, *Werk. u. Korr.* **9** (1972) 773.
11. R. C. HURST, M. DAVIES and P. HANCOCK, *Oxid. Metals* **9** (1975) 161.
12. M. P. MANAHAN, *J. Mater. Sci.* **25** (1990) 3424.
13. M. P. MANAHAN *et al.*, in "Mechanical Properties of Tube Scale from the Oconee-2 Steam Generator Using Miniature Specimens" (Final report from Battelle Columbus Division to Duke Power Company/MPR Associates, Inc., 23 December, 1986).
14. D. W. HAIRSTON and C. R. FRYE, in "Evaluation of Tube Deposits Oconee 2A OTSG Metallurgy Sample Number 244" (Duke Power Co. memo to R. W. Eaker, 14 May, 1985).
15. "Oconee II Sludge Dissolution Testing," Internal Report No. JBD1 (Final Report from Combustion Engineering-Windsor to Duke Power Co., April, 1986).
16. F. L. SINGER, in "Strength of Materials", C. Robichaud and T. R. Farrell (Harper Bros, New York, 1962) 6.2.
17. F. R. SHANLEY, in "Strength of Materials" (McGraw-Hill, New York, 1957) 16.11.
18. TIMOSHENKO and GOODIER, in "Theory of Elasticity", Edited by B. J. Clark and J. W. Maisel (McGraw-Hill, New York, 1970) ch. 4.
19. Z. SZLARSKA-SMIALOWSKA, in "Pitting Corrosion of Metals" (National Association of Corrosion Engineers, 1986).

Received 26 September 1988
and accepted 27 February 1989